KIR-HLA interactions extend human CD8$^+$ T cell lifespan in vivo

Yan Zhang[1]*, Ada W C Yan[2]*, Lies Boelen[2]*, Linda Hadcocks[1], Arafa Salam[1], Daniel Padrosa Gispert[2], Loiza Spanos[1,3], Laura Mora Bitria[2], Neda Nemat-Gorgani[4], James A Traherne[5], Chrissy Roberts[6], Danai Koftori[2], Graham P Taylor[2,7], Daniel Forton[1,8], Paul J Norman[4,9], Steven G E Marsh[10,11], Robert Busch[3]†, Derek Macallan[1]†, Becca Asquith[2]†

[1]Institute for Infection and Immunity, St George's, University of London, London, UK. [2]Department of Infectious Disease, Imperial College London, London, UK. [3]School of Life and Health Sciences, University of Roehampton, London, UK. [4]Department of Structural Biology and Department of Microbiology and Immunology, Stanford University School of Medicine, Stanford, CA, USA. [5]Department of Pathology, University of Cambridge, Cambridge, UK. [6]Department of Clinical Research, London School of Hygiene and Tropical Medicine, London, UK. [7]National Centre for Human Retrovirology, St Mary's Hospital, Imperial College Healthcare NHS Trust, London, UK. [8]Department of Gastroenterology and Hepatology, St George's University Hospitals NHS Foundation Trust, London, UK. [9]Department of Biomedical Informatics and Department of Immunology and Microbiology, University of Colorado School of Medicine, Aurora, CO, USA. [10]Anthony Nolan Research Institute, Royal Free Hospital, London, UK. [11]UCL Cancer Institute, UCL, London, UK.

* These authors contributed equally. †These authors contributed equally.
Corresponding author: Becca Asquith b.asquith@imperial.ac.uk Department of Infectious Disease, Imperial College London, London, W2 1PG, UK. +44(0) 207 594 3731.

All authors declare that they have no conflicts of interest.

Structured Abstract

Background. There is increasing evidence, in transgenic mice and in vitro, that inhibitory killer cell immunoglobulin-like receptors (iKIRs) can modulate T cell responses. Furthermore, we have previously shown that iKIRs are an important determinant of T cell-mediated control of chronic virus infection and that these results are consistent with an increase in $CD8^+$ T cell lifespan due to iKIR-ligand interactions. Here we test this prediction and investigate whether iKIRs affect T cell lifespan in humans in vivo.

Methods. We used stable isotope labelling with deuterated water to quantify memory $CD8^+$ T cell survival in healthy individuals and patients with chronic viral infections.

Results. We showed that an individual's iKIR-ligand genotype is a significant determinant of $CD8^+$ T cell lifespan: in individuals with two iKIR-ligand gene pairs, memory $CD8^+$ T cells survived on average for 125 days, in individuals with four iKIR-ligand gene pairs then memory $CD8^+$ T cell lifespan was doubled to 250 days. Additionally, we showed that this survival advantage is independent of iKIR expression by the T cell of interest and further that iKIR-ligand genotype altered $CD8^+$ and $CD4^+$ T cell immune aging phenotype.

Conclusions. Together these data reveal an unexpectedly large impact of iKIR genotype on T cell survival.

Funding. Wellcome Trust, Medical Research Council, EU Horizon 2020, EU FP7, Leukemia and Lymphoma Research, National Institute of Health Research Imperial Biomedical Research Centre, Imperial College Research Fellowship, National Institute of Health, Jefferiss Trust.

Introduction

The human killer cell immunoglobulin like receptors (KIRs) are a family of inhibitory and activating receptors. They are expressed predominantly by natural killer cells but are also found on T cells in a subset-specific manner(1, 2). Mice have functional analogues (the Ly49 receptors) but no orthologues, and there are significant differences between KIR and Ly49, both in structure and tissue distribution(3). The inhibitory KIR (iKIR) are characterised by long cytoplasmic tails, which contain immunoreceptor tyrosine-based inhibitory motifs (ITIMs) that, upon iKIR ligation, become phosphorylated and recruit tyrosine phosphatases(1). The ligands for the iKIR include HLA class I molecules, which they recognise in broad allotypes e.g. KIR2DL1 binds HLA C molecules carrying the C2 motif (lysine at position 80)(4-6). The presence of iKIR-ligand pairs is necessary for functional activity; however, iKIRs and their HLA ligands are encoded on different chromosomes and so are inherited independently. Therefore, within any given individual, not all iKIRs will necessarily have a matching ligand. In an individual carrying a particular iKIR gene as well as an HLA class I allele that can serve as its ligand (that is, an iKIR-ligand gene pair), we refer to that iKIR as "functional", (e.g. presence of *KIR2DL1* in

an individual positive for an *HLA C2* group allele). A "non-functional" iKIR is one that is carried in the absence of such a ligand (e.g. the presence of *KIR2DL1* in an individual negative for all *HLA C2* group alleles). Individuals differ in the number of functional iKIR genes they carry, which can vary between zero and four. Further complexity is added by allelic polymorphism of KIR genes, which affects protein structure thus affinity for HLA class I molecules, as well as protein expression(7).

We have previously found that the number of functional iKIR genes that a person carries significantly impacts $CD8^+$ T cell mediated control of viral infection(8). We investigated 11 well-documented, $CD8^+$ T cell-mediated HLA class I disease associations in human immunodeficiency virus (HIV-1), hepatitis C virus (HCV) and human T cell leukemia virus (HTLV-1) infections and found that, in every case, the HLA association was considerably stronger in individuals with a high number of functional iKIR genes than in individuals with a low number. We showed that this was true for both positive and detrimental HLA class I disease associations. Mathematical modelling showed that this apparently contradictory observation could be explained if iKIR-ligand interactions increased the survival of $CD8^+$ T cells(8).

This model prediction is consistent with the growing literature showing that, in iKIR transgenic mice and in human cells *in vitro*, iKIR ligation can indeed affect $CD8^+$ T cell survival(9-12). The underlying mechanisms can be divided into two groups which we refer to as direct and indirect (**Figure 1**). Both represent plausible explanations for the enhancement of HLA class I associations by functional iKIR which we have previously observed.

Under the direct mechanism (**Figure 1A**), ligation of iKIR expressed on the surface of T cells helps to protect that T cell from activation-induced cell death. This phenomenon was demonstrated by Ugolini *et al.* who showed that, in transgenic mice expressing a human iKIR (KIR2DL3) and its corresponding ligand (HLA-C*03), the iKIR-expressing T cells had a survival advantage that was absent in mice transgenic just for the iKIR or just for the HLA ligand(9). Consistent with this, human KIR^+ T cell clones have been shown to express high levels of the antiapoptotic molecule Bcl2(13). Furthermore, in vitro co-culture of activated human iKIR-expressing T cell clones with B cell lines expressing the corresponding cognate ligand promoted T cell survival, an effect that was blocked by both iKIR-specific antibodies and HLA class I-specific antibodies(8). However, previous studies suggest that iKIRs are only expressed on a relatively small proportion of predominantly late-differentiated T cells(2), raising doubt as to whether such large effects on HLA associations could be achieved through such a small subset of cells.

The indirect mechanisms (**Figure 1B**) comprise a broader set of pathways whereby iKIR expression on another cell (e.g. an NK cell or a different T cell) affects T cell lifespan. Mechanisms within this category include NK cell interactions with dendritic cells which subsequently affect T cell responses during priming(14), NK killing of activated $CD4^+$ and $CD8^+$ T cells(10-12) and suppression of T cells by a recently-described population of iKIR-expressing regulatory $CD8^+$ T cells(15, 16).

The aim of this study is to address three questions: 1) Do iKIRs increase $CD8^+$ T cell lifespan in humans *in vivo*? 2) If iKIRs do increase lifespan, then what is the size of the effect in humans? 3) Are the data most compatible with a direct or indirect mechanism?

Stable isotope labelling is the gold standard for investigating cell dynamics in humans(17-22). Here we used stable isotope labelling with deuterated water (^2H_2O) to quantify the in vivo survival of $CD8^+$ T central memory (T_{CM}) and effector memory T cells expressing CD45RA (T_{EMRA}) in individuals living with HIV-1, HCV or HTLV-1 as well as in uninfected controls(17, 23). We found that $CD8^+$ T cell survival is significantly affected by iKIR-HLA genotype (specifically, the number of functional iKIR genes) but not by iKIR expression on the measured T cell. Complementary genetic and immunophenotypic data showed additional evidence that iKIR-HLA genotype influences immune T cell ageing. Our results indicate that iKIR have a profound impact on T cell survival and are most consistent with an indirect pathway.

Results

1) iKIR expression on $CD4^+$ and $CD8^+$ T cells is low and not significantly increased by chronic virus infection

iKIR expression on T cells has previously been shown to be low in healthy individuals(2) but to be increased in untreated HIV-1 infection(24). We started by quantifying iKIR expression on T cells in our cohorts. Our first cohort ("Cohort 1", who subsequently participated in labelling studies) consisted of individuals with treated HIV-1 infection (all with low, often undetectable viral load; N=7), viraemic untreated chronic HCV infection (N=9), and chronic HTLV-1 infection (N=3), as well as uninfected individuals (N=4). We quantified the proportion of $CD4^+$ and $CD8^+$ T cell subsets that expressed KIR2DL1, KIR2DL2/L3 and KIR3DL1 by flow cytometry and identified the factors associated with iKIR expression (Methods, **Supp Figure 1**).

In general, we observed low iKIR expression across T cell subsets (median 4.7% for $CD8^+$ T cells, 0.3% for $CD4^+$ T cells), although expression varied markedly between individuals. To identify determinants of iKIR expression on T cells, multivariate stepwise regression was

performed with the following predictors: age, gender, CMV serostatus, cell phenotype (CD4, CD8), T cell differentiation status (as an ordinal), infection status (uninfected, HIV-1, HTLV-1, HCV) and iKIR (KIR2DL1, KIR2DL2/L3, KIR3DL1). We found that iKIR expression increased significantly with cell differentiation stage ($P=4x10^{-14}$), was higher for KIR2DL2/L3 than KIR2DL1 ($P=4x10^{-12}$) and higher for $CD8^+$ T cells than $CD4^+$ T cells but was not significantly increased by viral infection (either when considered separately or when pooled to increase power); **Figure 2**, **Supp Table 1, Supp Table 2**. The lack of association between iKIR expression and HIV-1 status and HTLV-1 status was perhaps not unexpected since the HIV-1 infected subjects were aviraemic (on antiretroviral treatment) and HTLV-1 infection is known to be largely latent(25). However, we were surprised that iKIR expression by T cells was not elevated in the HCV-infected participants who were all chronically viraemic. To verify this absence of an effect of HCV infection, we recruited a second, larger independent cohort ("Cohort 2") consisting of 33 uninfected controls and 15 individuals living with HCV and repeated the analysis. Results were very similar to our findings in the first cohort, with cell differentiation stage ($P=4x10^{-17}$), CD8 phenotype (P=0.002) and KIR2DL2/3 ($P=7x10^{-35}$) all significant predictors of high iKIR expression. HCV infection and CMV infection remained nonsignificant (P=0.2, P=0.7 respectively); **Supp Figure 2, Supp Table 2**.

Our results confirm previous findings(2) that only a minority of T cells express iKIR in healthy individuals and extend them showing that iKIR expression remains low in individuals with chronic virus infection.

2) iKIR-ligand genotype strongly determines T cell lifespan in vivo

To assess the impact of iKIR on $CD8^+$ T cell survival in vivo we used stable isotope labelling. Individuals in Cohort 1 (N=23, above) received 7 weeks of deuterated "heavy" water (^2H_2O, Methods); serial saliva and blood samples were taken during and up to 112 days after the start of labelling. Monocytes were extracted as a rapidly turning over reference population (Methods; **Supp Figure 3, Supp Figure 4, Supp Figure 5, Supp Table 3**). The remaining peripheral blood mononuclear cells were FACS sorted into $CD8^+$ T central memory (T_{CM}) and $CD8^+$ T effector memory RA revertant (T_{EMRA}) on the basis of cell surface expression of canonical T cell differentiation markers (T_{CM}: $CD45RA^-CD28^+$ T_{EMRA}: $CD45RA^+CD28^+$). For all individuals, KIR and HLA genotype was determined prior to sorting allowing us to establish bespoke individual gating strategies. This enabled us to further sort both CD8 subsets into cells (T_{CM} or T_{EMRA}) expressing a functional iKIR (i.e. an iKIR whose corresponding ligand was encoded by the individual's HLA alleles) and cells expressing a nonfunctional iKIR (an iKIR in an individual who was negative for all HLA alleles encoding the corresponding ligands). When cells expressing a non-functional iKIR were not available (due to low or absent cell frequencies) then cells which were iKIR negative were collected instead; (**Supp Figure 1B**).

Deuterium enrichment in the DNA of monocytes and sorted T cell subpopulations was measured by gas chromatography/mass spectrometry(23). Mathematical models were fitted to the data in order to estimate the lifespan of the different T cell subsets (**Figure 3, Figure 4, Supp Table 4**, Methods).

The aim of the study was three-fold: i) to test whether iKIR (expression or genotype) were a determinant of T cell survival ii) to quantify the impact of iKIR on T cell lifespan and iii) to investigate which of the two pathways, direct or indirect, was most likely. The study was designed so that the two different pathways (summarised in **Figure 1**) would give two quite distinct patterns to the data, **Figure 5A-D**. If the direct pathway operates, in which iKIR expressed directly on a $CD8^+$ T cell increases that particular T cell's lifespan when ligated (**Figure 1A**) then, in a paired, within-individual study we would predict that the cells expressing a functional iKIR would live for longer than cells that were iKIR-negative or expressing a non-functional iKIR, **Figure 5A**. But looking between individuals we would predict no relationship between iKIR genotype (specifically the number of iKIR-HLA ligand pairs carried by the individual) and T cell lifespan. This is because the data includes measurements not just of cells expressing functional iKIR but also of cells that express no iKIR and cells that express non-functional iKIR both of which would obscure any signal coming from cells expressing functional iKIR. Furthermore, even within those populations of cells which express a functional iKIR, there is no reason to expect a positive correlation (i.e., given that a cell expresses a functional iKIR, there is no reason to expect number of functional iKIR genes to affect its lifespan further), **Figure 5B**. Conversely, if an indirect mechanism dominates (**Figure 1B**) then iKIR expression on the measured $CD8^+$ T cell would be irrelevant and so we would predict that there would be no relationship between functional iKIR expression and cell survival within-individuals, **Figure 5C**, but when we look between-individuals then we would predict that the number of iKIR-ligand gene pairs carried by the individual would be positively correlated with $CD8^+$ T cell lifespan, **Figure 5D**. Previous work has shown that different CD8 memory/effector T-cell subsets have different lifespans (17); thus, in order to rule out confounding effects of memory/effector differentiation, the analysis was performed for matched subsets.

Expression of a functional iKIR is not a significant predictor of $CD8^+$ T cell lifespan (within-individual comparison): First we investigated whether a $CD8^+$ T cell's lifespan was influenced by its expression of functional iKIR (i.e. iKIR expression where one or more alleles encoding the ligand were carried by the individual). We estimated the lifespan of a total of 54 T cell subsets from 18 individuals (**Figure 3, Figure 4, Supp Table 4**) and assessed whether T_{CM} and T_{EMRA} expressing a functional iKIR had longer lifespan than matched T_{CM} and T_{EMRA} from the same individual expressing only nonfunctional iKIR or that were iKIR-negative. We found no

evidence that T cell lifespan was dependent on functional iKIR expression (*P*=0.79, Wilcoxon two tailed; **Figure 5E**). Repeating the analysis excluding the iKIR-negative T cells did not change the conclusion (P=0.82, Wilcoxon two tailed). Furthermore, a multivariate regression to test if expression of a functional iKIR predicted the T cell lifespan (with covariates: cell subpopulation [T_{CM} or T_{EMRA}], infection status [HIV-1/HCV/HTLV-1/control]) also showed that expression of one or more functional iKIR was not a significant predictor of T cell lifespan (*P*=0.34, linear multivariate regression, **Supp Results 1, Supp Table 5A**).

Count of iKIR-ligand gene pairs is a highly significant predictor of CD8$^+$ T cell lifespan (between-individual comparison): Next, we investigated whether, between individuals, an individual's iKIR and HLA genotype (specifically the count of iKIR – HLA ligand gene pairs in their genome) was a significant predictor of T cell lifespan. In linear multivariate regression (with covariates: cell subpopulation [T_{CM} or T_{EMRA}], infection status [HIV-1 /HCV /HTLV-1 /control]) the count of iKIR-ligand gene pairs was a significant determinant of T cell survival, **Figure 5F** (Est= +0.41, P= 3.4×10^{-6}; N=54 T cell subsets from 18 individuals, **Supp Results 2**, **Supp Table 5B**). As well as being highly statistically significant, the size of the effect was striking: in an individual with two iKIR-ligand pairs in their genome, then after correcting for viral infection and cell phenotype (i.e. for the baseline of T_{CM} cells in an uninfected individual), their memory CD8$^+$ T cells lived, on average, for 125 days; in contrast, in an individual with four iKIR-ligand pairs in their genome, then their memory CD8$^+$ T cells lived for 250 days, a doubling in survival. Inclusion of the covariates age, gender, CMV serostatus and viral load did not change this conclusion. We had excluded from this analysis any individuals carrying alleles encoding the classical KIR3DL2 ligands (HLA-A*03 and HLA-A*11), as there is evidence that the behaviour of KIR3DL2, a framework KIR with an additional ITIM motif in its cytoplasmic tail, might be different from that of the other iKIRs(26-28). When we included these individuals, the overall conclusions were unchanged, but the size of the effect was slightly smaller (Est= +0.38, P=2×10^{-5}), consistent with the idea that KIR3DL2 is distinct from the other inhibitory KIR. Previously we have also used inhibitory score (the count of functional iKIR weighted by strength of the KIR:ligand interaction) as a predictor. Here, the count and the score (which are strongly correlated) performed similarly and there was no significant benefit of one compared to the other (P=0.09, Davidson-MacKinnon J test, **Supp Results 3**). In contrast, counting only the number of iKIR, without considering the presence of the ligand, performed significantly worse (P=9×10^{-5}, Davidson-MacKinnon J test, **Supp Results 3**), indicating that ligation of the iKIR is essential for the increase in T cell lifespan.

Comparing the results (**Figure 5E,F**) with the predictions of the two different pathways (**Figure 5A,B** and **Figure 5C,D**) it can be seen that the observed impact of iKIR expression and genotype on T cell survival is most consistent with the indirect pathway.

One possible caveat to this conclusion in favour of the indirect pathway was if cells upregulated and down-regulated iKIR rapidly during the course of the labelling experiment, then, cells sorted ex vivo as expressing functional iKIR might actually have been iKIR negative or expressing a non-functional iKIR in vivo and vis versa. This could potentially disguise any association between T cell lifespan and functional iKIR expression between individuals. However, the proportion of T_{CM} and T_{EMRA} that express functional iKIR is low (see section 1 above). We calculate that, for differences in this small population of T cells (median 6% of T_{CM} and T_{EMRA}) to be responsible for the doubling in bulk T cell lifespan seen between individuals, then iKIR expression would need to increase survival of this minority population by nearly 20-fold (**Supp Results 4**). Furthermore, as argued above, we would not expect the direct pathway to generate a correlation between functional iKIR count and $CD8^+$ T cell lifespan. In particular, the fraction of $iKIR^+$ $CD8^+$ T cells would need to be significantly positively correlated with the number of iKIR-ligand gene pairs, which we did not observe (Rs= -0.08, P=0.77, data not shown). Similarly, there was no strong correlation between the fraction of $CD8^+$ T cells expressing a functional iKIR and the number of iKIR-ligand gene pairs (Rs= +0.23, P=0.42, data not shown). These observations further support the suggestion that the indirect rather than the direct mechanism is operating.

3) iKIR expression and T cell activation.

We also investigated Ki67 expression in Cohort 2 as a complementary approach to assess the relationship between iKIR expression and proliferation. We found significantly higher levels of Ki67 expression in $iKIR^+$ T cell subsets, when compared with corresponding $iKIR^-$ cells, regardless of whether the iKIR was functional or not (**Supp Figure 6**). We considered two possible explanations for this observation. The first, that $iKIR^+$ cells are dividing more rapidly than $iKIR^-$ cells, the second that iKIR expression is upregulated transiently in proliferating / activated cells. The first interpretation is inconsistent with the in vivo labelling data. We therefore explored the relationship between iKIR expression and T cell activation in vitro. We showed that iKIR expression was indeed significantly upregulated on $CD8^+$ T cells following stimulation with αCD3αCD28, that iKIR expression was higher on activated ($CD38^+$) cells than quiescent cells ($CD38^-$) and that iKIR expression was stable at a cellular level for at least 72hrs; **Supp Figure 7, Supp Figure 8, Supp Figure 9**. This is consistent with work showing upregulation followed by slow downregulation of iKIR on human T cell clones following activation(29).

4) Relationship between count of iKIR-ligand gene pairs and CD57 expression

Intuitively, one would expect that in individuals with a high number of iKIR-HLA ligand pairs (i.e. a high functional iKIR gene count), where the survival of $CD8^+$ T cells is elevated, then the

average age of a $CD8^+$ T cell would be increased. This intuition was confirmed by mathematical modelling, which predicts a weak relationship between cell survival (and thus iKIR/HLA genotype) and cell age (defined as the time between a cell entering the memory compartment and sampling, Methods). To test this prediction, we first looked for a cell phenotype that is correlated with cell age. It has been reported that expression of CD57, a terminally sulfated glycan carbohydrate epitope, is increased as cells age, though it is not a marker of replicative senescence(30, 31). To test if CD57 expression can be considered a valid surrogate for cell age we turned to the UK Adult Twin Register (TwinsUK), a large cohort of monozygotic and dizygotic twins. In a subset of this cohort (N=333), immune phenotypes have been quantified by flow cytometry alongside metadata, including age(32). We found evidence for a positive correlation between age and the proportion of $CD8^+CD45RA^+$, $CD8^+CD45RA^-$, $CD4^+CD45RA^+$ and $CD4^+CD45RA^-$ cells that were $CD57^+$ (Spearman test $P=6x10^{-9}$, 0.06, $4x10^{-5}$, 0.0002 respectively). Although this correlation is between CD57 expression and an individual's age rather than cell age per se, the two are likely to be linked and henceforth we use the proportion of cells expressing CD57 as a surrogate of that population's age.

On this basis, we predict that, in individuals where the functional iKIR count is high the proportion of cells expressing CD57 will be high and that the effect would be most pronounced in older individuals, where the impact of iKIR genotype on cell age would have had longest to accumulate. We therefore recruited a cohort of 63 healthy older adults (age ≥60 yrs, Cohort 3) and analysed the proportion of naïve/T_{SCM}, early T_{CM} and late T_{CM} (also called transitional memory), T_{EM} and T_{EMRA} $CD8^+$ and $CD4^+$ cells expressing CD57 by flow cytometry, **Supp Figure 10**. We performed multivariate linear regression with independent variables functional iKIR gene count, CMV serostatus, age and cell differentiation state. We found that for $CD8^+$ T cells, CD57 expression was significantly associated with functional iKIR count (**Figure 6,** P=0.003), with the percentage of cells expressing high levels of CD57 increasing by 3% (β=0.03, **Supp Table 6**) for each additional functional iKIR in a person's genome. To put this into context, the same magnitude of increase in CD57 positivity (3%) is seen with an increase in an individual's age of 12yrs. If naïve and T_{CM} cells (which express very low levels of CD57) were excluded, then the results were even more striking (P=0.0005, 7.8% increase for each additional functional iKIR gene, **Supp Table 7**). For $CD4^+$ cells the same trend was seen, but the effect size was smaller (an increase of 2% for each additional functional iKIR gene) and not significant (P=0.1, **Supp Table 6**). Focussing on the T cell subpopulations with sufficient numbers of $CD57^+$ events for accurate analysis (median≥150 events), namely $CD8^+$ T_{EM}, $CD8^+$ T_{EMRA} and $CD4^+$ $T_{EM,}$ then we find significant associations between CD57 expression and functional iKIR count in each case (P=0.018, P=0.012, P=0.036 respectively), **Figure 6** We conclude that our prediction that $CD8^+$ T cells will be "older" in people with a high number of

functional iKIR genes is consistent with the data. Independent of this interpretation that CD57 expression reflects T cell age, these data show that functional iKIR gene count affects both $CD8^+$ and $CD4^+$ T cell immunophenotype.

Discussion

In this study we show that the number of iKIR-HLA ligand gene pairs that an individual carries in their genome is a significant predictor of the lifespan of their memory $CD8^+$ T cells. As well as being highly statistically significant ($P=3x10^{-6}$), the size of the effect was striking: we found that $CD8^+$ cell lifespan increased by approximately 60 days for each additional functional iKIR gene that a person possessed, resulting in a doubling in T cell survival for a person with four functional iKIR genes compared to someone with two functional iKIR genes. Although our previous work had anticipated that iKIR-HLA ligand interactions would increase T cell survival, we still found the size of the effect to be unexpectedly large. There are two reasons why such a large effect is striking. First, the variable we are considering, count of functional iKIR genes, is purely genetic information and considers only two gene families (KIR and HLA), a very large number of other factors, both genetic and environmental, would be expected to impact on T cell kinetics and to obscure the relationship. The fact that the effect was readily evident despite such variance emphasises its importance. Second, the genes we consider are, first and foremost, genes that regulate innate immunity, that they have such a marked impact on adaptive T cell survival is remarkable.

A number of pathways by which functional iKIR could enhance $CD8^+$ T cell lifespan have been described in the literature. We divide these into “direct” and “indirect” pathways (**Figure 1**). The patterns we observe in the data, in particular the strong correlation between functional iKIR count and $CD8^+$ T cell lifespan and the absence of any discernible effect of functional iKIR expression on a cell’s lifespan, argue in favour of an indirect mechanism (**Figure 5**). The direct and indirect mechanisms are not mutually exclusive, and, given the existing data suggesting that KIR expression can directly affect a cell’s survival in vitro and in mice, it is plausible that this does also occur in humans but the magnitude of the effect is not discernible in our hands and we suggest that the indirect pathway rather than the direct pathway is the more important determinant of $CD8^+$ T cell lifespan in humans in vivo.

We also found that an individual’s functional iKIR gene count had a significant impact on immune aging, specifically on CD57 expression. CD57 expression is often considered a marker of immune aging though we have previously shown it is not a marker of replicative senescence(31). In this current study we showed that CD57 expression was significantly

positively correlated with functional iKIR count for $CD8^+$ T cells but also for $CD4^+$ T cells: hinting that functional iKIR might also impact $CD4^+$ T cells. Independent of this interpretation, these data point to another important way in which functional iKIR gene count modulates immunophenotype. Whether iKIR modulate other aspects of T cell dynamics such as clonal evolution and diversity is an open question.

We found that iKIR-expressing T cells had higher levels of Ki67 expression than iKIR-negative T cells but, by stable isotope labelling, there was no difference in the proliferation rates of iKIR-positive and iKIR-negative cells measured in the longer term. We suggest that Ki67 and iKIR are transiently upregulated upon activation (consistent with our data as well as previous observations(29)) but that, over a longer time scale (49 days of the label administration, about 110 days observation), iKIR expression is not associated with differences in T cell proliferation. That is, Ki67 is better considered as a timestamp of a recently proliferated cell (33). This serves as a caveat against the interpretation of Ki67 as a measure of in vivo lifespan and emphasises the importance of direct in vivo measurements such as those made using stable isotopes. This conclusion is echoed by animal studies which also found substantial differences between Ki67 expression and more direct measures of cell proliferation(34).

We suggest that together these data provide a mechanistic explanation for our previous observations that an increased number of iKIR-HLA ligand gene pairs significantly enhances $CD8^+$ T cell-mediated control of virus in HIV-1, HCV and HTLV-1 infections. Mathematical modelling showed that these observations could be explained if iKIR-ligand interactions increased the survival of $CD8^+$ T cells(8). Furthermore, in a longitudinal HIV-1 infected cohort, this previous work also showed that protective *HLA-B*57* and detrimental *HLA-B*35Px* associations were both better maintained over time in people with a high number of functional iKIR genes compared to people with a low number; again consistent with the hypothesis that the enhancement of HLA associations observed related to increased T cell survival. Very recently, we have found that the number of functional iKIR genes also impacts HLA associations with the risk of type 1 diabetes (Mora Bitria/Asquith unpublished observations), suggesting that the process we have identified in the context of chronic viral infection is also relevant in some cases of autoimmunity. Although it is very early to be speculating about therapeutic implications, two facts are pertinent. Firstly, that this pathway is clinically relevant and secondly that this pathway is druggable. Monoclonal antibodies (mAb) that are capable of blocking or of activating iKIR in vitro have been developed. Lirulimab, a mAb that blocks KIR2DL1 and KIR2DL2/L3, has been developed as an NK therapeutic and tested in human clinical trials to treat solid tumors and hematologic malignancies(35); it could potentially be repositioned to alter T cell lifespan. Some indirect mechanisms e.g. an impact of iKIR on NK cell education may be harder to drug as the effects

may have already occurred during development, nevertheless the requirement for NK signalling must still be met for effector function and can potentially still be targeted. In the long term there is, therefore, the possibility to modulate T cell responses in vivo by dampening (by KIR blocking) or boosting (by KIR ligation) T cell survival depending on context.

Another potentially important direction for translation is in allo-hematopoietic stem cell transplant donor-recipient matching. Several studies have already considered the impact of donor KIR genotype and donor-recipient KIR ligand mismatches on NK cell alloreactivity(36-38). Our work suggests that donor NK cell autoreactivity may also be relevant. An essential prerequisite for translation is a detailed understanding of the underlying mechanism. For this an animal model would be invaluable. The extent to which murine Ly49 receptors adequately model human iKIR is unclear. One step would be to see whether the relationship we observe between count of functional iKIR genes and $CD8^+$ cell lifespan in humans is recapitulated by murine models.

One limitation of this study is that the "count of functional iKIR genes" that we use is relatively simple and does not incorporate iKIR allele-level information (other than the broad allotypes of KIR2DL2/L3 and KIR3DL1/S1). There are two main reasons for the decision. First our aim was to investigate possible mechanisms underlying our prior observation that functional iKIR count enhanced HLA class I associations with clinical outcome and so we needed to use this previous definition of functional iKIR count (which did not include allele level information) for comparability. Second, it is far from clear how allele level information should be incorporated into the functional count: should some alleles count as less than 1? If so, which alleles and what count should they be assigned? Should the "count" of a KIR-HLA allele pair only reflect its strength of signalling or should other factors such as expression level of KIR and HLA also be incorporated? Our first attempt at incorporating some of these details (the weighted inhibitory score) was also a significant predictor of $CD8^+$ T cell lifespan but it did not perform better than the unweighted count of functional iKIR genes. In stark contrast, a count of the number of iKIR genes, without taking into account whether or not they were functional, performed very poorly as we expected, suggesting that, though simple, there is content in our definition of a functional iKIR gene. Ultimately, a much larger study would be needed to interrogate such subtleties in the future.

To summarise, the data presented here show that iKIR-HLA ligand genotype has a profound impact on $CD8^+$ T cell lifespan as well as on $CD4^+$ and $CD8^+$ T cell immunophenotype. Furthermore, since these are relationships between genotype and phenotypes, the direction of causality is unequivocal. Separately, we have also shown that iKIR-ligand genotype has direct and measurable consequences for human health: impacting on the risk of developing type 1 diabetes, the rate of progression to low $CD4^+$ count in people living with HIV-1, the

odds of spontaneous clearance of HCV and the risk of developing inflammatory disease in the context of HTLV-1 infection. The wide range of diseases involved, and the central role of T cells in human immunity, suggest that this iKIR impact on $CD8^+$ T cell lifespan may be of fundamental importance.

Methods

EXPERIMENTAL DATA

Study participants

A total of 134 subjects across three cohorts were recruited:

Cohort 1 (KIR expression analysis and stable isotope labelling). 23 healthy adults were recruited, the cohort consisted of uninfected controls (N=4), individuals living with viremic untreated HCV (N=9), individuals living with aviremic treated HIV-1 (N=7) and individuals living with untreated HTLV-1 (N=3). Individuals with no functional iKIR were excluded from the study (as we needed some functional iKIR expression to investigate the direct hypothesis). For the analysis of labelling, individuals carrying a KIR3DL2 ligand were initially excluded (see below) leaving 18 individuals.

Cohort 2 (KIR expression analysis - replication cohort). 48 healthy adults were recruited, the cohort consisted of uninfected controls (N=33) and individuals living with viremic untreated HCV (N=15). Hepatitis C viral loads ranged from $2.4x10^4$ to $3.3x10^6$ with a median of $1.8x10^6$ RNA copies/ml. All individuals in cohort 2 were seronegative for HIV-1 infection.

Cohort 3 (CD57 expression analysis). We recruited 63 healthy older adults (≥ 60 years of age, range 60-91, median 75 years). All were seronegative for HIV-1, Hepatitis B and C infection.

KIR expression analysis

For analysis of Cohort 1, $CD4^+$ and $CD8^+$ T cells were gated into four subpopulations: Naïve/T_{SCM} (naïve/ T stem cell like-memory: $CD45RA^+CD28^+$), T_{CM} (central memory: $CD45RA^-CD28^+$), T_{EM} (effector memory: $CD45RA^-CD28^-$) and T_{EMRA} (CD45RA-expressing late effector memory: $CD45RA^+CD28^-$); see Supplementary Methods for panel details including clone names and **Supp Figure 1A** for representative gating. iKIR antibodies specific for KIR2DL1, KIR2DL2/L3 and KIR3DL1 were conjugated to different dyes enabling analysis of co-expression and analysed and sorted on a FACS Aria III (BD Biosciences, Reading UK). Cytometry data were quantitated using FlowJo (LLC, Ashland, Oregon).

For analysis of Cohort 2, T cell subpopulations were defined as above. PE-conjugated iKIR-specific antibodies were used to stain samples separately for each iKIR studied. Cells were analysed on a BD Canto II cytometer (BD Biosciences) and data quantified using FlowJo.

CD57 expression analysis

$CD4^+$ and $CD8^+$ T cells were gated as above. To permit higher resolution, T_{CM} were further separated into early T_{CM} and late T_{CM} (also called transitional memory, T_{TM}(39)) by CCR7 staining. For enumeration of highly-differentiated cells, staining with CD57 was used (see **Supp Figure 10** for representative gating).

Stable isotope labelling in vivo.

We have previously described the labelling protocol in detail(40). Briefly, participants were given oral doses of 70% deuterated water (^2H_2O) over a 7-week period (50 ml three times daily for one week, then twice daily thereafter). Saliva samples were collected for evaluation of body water labelling. Peripheral blood was collected at successive time-points during and after labelling and peripheral blood mononuclear cells (PBMC) separated by Ficoll gradient centrifugation. Monocytes for normalisation, as a cell population expected to reach fully-labelled status during the labelling phase, were sorted from an aliquot of PBMC by CD14 magnetic bead column positive selection (MACS, Miltenyi Biotech, Bisley, UK). PBMC were sorted using a BD FACSAria III flow cytometer into $CD8^+$ T central memory (T_{CM}) and $CD8^+$ T effector memory RA revertant (T_{EMRA}) on the basis of cell surface expression of canonical differentiation markers (T_{CM}: $CD45RA^{-}CD28^+$ T_{EMRA}: $CD45RA^+CD28^-$). Both subsets were further sorted on the basis of their iKIR expression into cells (T_{CM} or T_{EMRA}) expressing a functional iKIR and cells expressing a nonfunctional iKIR (if the latter were not available or cell numbers were too low, then cells which were iKIR negative were collected instead). Each individual had a bespoke gating strategy based on their HLA and KIR genotype as each individual had different iKIR which were functional and nonfunctional. Due to low or absent cell frequencies, it was not possible to collect all cell populations for all individuals; see **Supp Figure 1A&B** for representative gating . Deuterium enrichment in the DNA of monocytes and sorted T cell subpopulations was measured by gas chromatography/mass spectrometry of the pentafluorobenzyl derivative as previously described(23, 41).

Definition of functional and non-functional iKIR expression. We used the following rules to define cells expressing functional and non-functional iKIR. A cell was classified as expressing a functional iKIR if it expressed any of KIR2DL1, KIR2DL2/L3 and/or KIR3DL1 and the individual was positive for any HLA allele encoding a corresponding ligand (KIR2DL1: *C2*. KIR2DL2: *C1* (which includes *HLA-B*46* and *-B*73*), *C2*. KIR2DL3: *C1* (including *HLA-B*46* and *-B*73*). KIR3DL1: *Bw4* (which includes *HLA-A*23, -A*24, -A*32* together with some other rare HLA-A alleles), using the definitions of iKIR ligands provided in the Immuno Polymorphism Database(4, 42)). A cell was classified as expressing a non-functional iKIR if it both (i) expressed an iKIR (KIR2DL1, KIR2DL2/L3 and/or KIR3DL1) for which the individual did not carry an allele encoding any corresponding HLA ligand and (ii) did not express any functional iKIR (that is we assumed that the signal for a functional iKIR was dominant, and this cell would instead be classified as expressing a functional iKIR).

In the case where KIR2DL2 was functional and KIR2DL3 was non-functional then cells expressing KIR2DL/L3 could not be unambiguously classified (as either functional or non-functional) and so were not collected.

There is evidence that KIR3DL2, a framework KIR, behaves differently to the other iKIR particularly the exceptionally strong binding to HLA-B*27 heavy chain homodimers and non-HLA ligands(2, 26-28, 43, 44) and we were concerned it may confound our results. Therefore, for donors negative for the alleles encoding HLA ligands of KIR3DL2 (*HLA-A*03*, *A*11*, *B*27*), cells expressing KIR3DL2 were excluded from the sorted populations (directed into the dump channel); whilst donors who were positive for any of the alleles encoding HLA ligands of KIR3DL2 (N=5) were removed from the analysis in the first instance, reducing the cohort size from 23 to 18. For the sensitivity analysis including those individuals positive for the classical KIR3DL2 ligands *HLA-A*03* and *-A*11*, (N=2) then cells negative for KIR3DL2 were included and classified with the standard definitions (non-functional or iKIR-negative); cells in other individuals kept their original classifications.

In vitro activation studies.

PBMC from 10 healthy donors were either cultured in media alone or were stimulated with purified anti-human plate bound CD3 and soluble CD28 (2µg/ml and 1µg/ml respectively, BD Biosciences). Expression of iKIR and CD38 on $CD8^+$ cells was measured by flow cytometry at 6, 12 and 24h. For iKIR expression, a cocktail of PE-conjugated KIR2DL1, KIR2DL2/L3 and KIR3DL1 specific antibodies were used. To assess the stability of iKIR expression, PBMC were stimulated as above, sorted into the $iKIR^+$ and $iKIR^-$ fraction and allowed to rest for 72h. iKIR expression was evaluated by flow cytometry at the time of sorting (0h) and at 72h.

Genotyping.

High resolution HLA typing for the HLA-A, B and C loci was carried out by the Antony Nolan Trust using next generation sequencing. KIR genotyping of Cohort 1 was performed by the qKAT multiplex qPCR method using a Roche LightCycler 480(45); KIR genotyping of Cohort 2 was performed by PCR-SSP following Vilches et al(46) and KIR genotyping of cohort 3 was performed by high throughput sequencing(47) and interpreted using the bioinformatics pipeline PING(48).

MATHEMATICAL MODELLING

Fitting the stable isotope labelling data.

There are three parts in the model to estimate the proliferation and disappearance rate of the T cell subsets. First, we quantify the availability of label in body water by measuring the fraction of heavy water in the saliva. We describe this availability with an empirical function *S(t)* with three parts (1) to reflect the three part protocol (full dose 7 days, 2/3 dose 42 days, delabel) (**Supp Figure 3**). Individuals were assumed to have different values of f but δ was constrained to be the same for everyone (since turnover of body water is expected to be similar between individuals). Replacing the empirical function with a piecewise function gave very similar results.

$$S(t)= \begin{cases} f(1-e^{-\delta t}) & t \le 7 \\ \frac{2}{3} f(1-e^{-\delta(t-7)}) + f(1-e^{-\delta 7})e^{-\delta(t-7)} & 7 < t \le 49 \\ \left[\frac{2}{3} f(1-e^{-\delta(49-7)}) + f(1-e^{-\delta 7})e^{-\delta(49-7)}\right] e^{-\delta(t-49)} & t > 49 \end{cases} \quad (1)$$

Next, for each individual we model the fraction of label in a rapidly turning over population (monocytes) in order to estimate the amplification factor b_w (also referred to as c(21)); this is a factor that reflects the increase in M+1 when a cell divides given enrichment $S(t)$ i.e. it scales between label enrichment in newly synthesised DNA and precursor availability in body water(17). We describe the label enrichment in DNA of monocytes using a mechanistic model (2) previously proposed(19, 49)

$$\begin{aligned} \dot{L}_M &= p_m b_w S(t) - r_1 L_M \\ \dot{L}_B &= r_1 L_M (t-\Delta)\frac{M}{B} - r_2 L_B \end{aligned} \quad (2)$$

Where L_M is the fraction of label in bone marrow monocyte precursors, L_B is the fraction of label in blood monocytes (the observable), p_m is the proliferation rate of precursors, r_1 is the rate of exit from the mitotic pool in bone marrow, Δ is the time spent in the post-mitotic pool in bone marrow, M/B is the ratio of the number of monocytes in the bone marrow to the number of monocytes in the blood, $S(t)$ is the saliva enrichment estimated for that individual in step 1 and b_w is the amplification factor of interest, **Supp Figure 4**. We use equilibrium constraints to eliminate p_m and r_1. M/B and Δ were fixed at estimates of 2.6 and 1.6 days respectively(19, 49) (however, we showed that the estimates of b_w are independent of these values; this follows because b_w depends only on the plateau enrichment in blood monocytes). There were therefore two free parameters (b_w and r_2) which were estimated by fitting the model to the data; different values were allowed for each individual and we used uniform priors of [0,7] and [0,10] for b_w and r_2 respectively. Finally, we use the information from steps 1 and 2 to describe the label enrichment in T cells. The equations for the fraction of label in T cells are given in (3)

$$\begin{aligned} \dot{L} &= p b_w S(t) - d^* L \\ O(t) &= L(t-\Delta_L) \end{aligned} \quad (3)$$

Where L is the fraction of label in the DNA of the T cell subset at the site of division, p is the proliferation rate of T cells, $S(t)$ the saliva enrichment estimated in step 1 above, b_w the amplification factor estimated in step 2 above, d^* the disappearance rate of labelled T cells, $O(t)$ the observed label at time t which is the label at the site of division (likely lymphoid tissue) lagged by a time Δ_L to reflect a delay of Δ_L days for a T cell to traffic from the site of division to the blood (where it is observed). The parameters p, d^* and Δ_L are drawn, for each T cell subset, from a lognormal prior distribution whose parameters are fitted (i.e. a hierarchical

model). The lognormal distribution has two parameters μ and σ. The prior for σ_p, σ_{d^*} and $\sigma_{\Delta L}$ is uniform between 0 and 1. The priors for μ_p, μ_{d^*} and $\mu_{\Delta L}$ are uniform between $-\infty$ and log(0.05), log(1) and log(21) respectively. Using a hierarchical model improved convergence compared to allowing parameters to vary freely. Note that the hyperparameter μ_p is the same for all lymphocyte populations regardless of infection status, functional iKIR count, cell subpopulation ($CD8^+$ T_{CM} or T_{EMRA}) and iKIR expression status (functional, non-functional, iKIR negative); i.e at no point do we impose any assumptions on how *p* varies between the populations. Equation (3) was solved analytically to speed up the fitting process. All model fitting was conducted using a Bayesian framework, using the NUTS sampler implemented in Stan (via the R package rstan(50)). The saliva, monocyte and lymphocyte data were fitted simultaneously across all individuals and lymphocyte subsets. Simultaneous fitting of saliva, monocyte and lymphocyte data means that errors are propagated correctly (fitting in a stepwise manner , as is common (21) ,with point estimates from the first step being used in the second step and so on will lead to an underestimate of errors on the final parameters). To summarise, the parameters f, δ, b_w, r_2, p, d^* and Δ_L were fitted; f, b_w and r_2 were allowed to be different for each individual, p, d^* and Δ_L were allowed to be different for each individual and each population, δ was constrained to be the same for all individuals, the total number of data points was 1,085 (not including replicates, typically 3 per data point). Best fits of the model to the saliva and monocyte data are shown in **Supp Figure 3** and **Supp Figure 5** respectively, best fits of the model to the T cell data are shown in **Figure 3** and **Figure 4.** Parameter estimates are provided in **Supp Table 3** and **Supp Table 4**. Model fitting code is provided at https://github.com/ada-w-yan/kirdynamics. Repeating the fits in a frequentist framework using the global optimiser pseudo from the package FME(51) in R v 4.1.2 gave virtually identical results. Cell lifespan we report is the average for each subpopulation, it is defined as $1/p$; it is the average time between creation of a cell (by proliferation) and loss of the cell (by proliferation, death, differentiation); it differs from half-life by a factor of ln(2) i.e. $half\ life = ln(2).lifespan = ln(2)/p$.

Model prediction of the relationship between cell survival and cell age

We calculate how a change in memory $CD8^+$ T cell lifetime would impact $CD8^+$ T cell age. We model the turnover of $CD8^+$ T cells as

$$\frac{dz}{dt} = \lambda + sz\left(1 - \frac{z}{k}\right) - \mu z \tag{4}$$

where z is the concentration of $CD8^+$ T cells, λ is the rate at which cells enter the memory T cell compartment, s is the rate of division, k is the carrying capacity of $CD8^+$ T cells, and μ is the death rate.

The lifetime of CD8⁺ T cells in this model, as measured by stable isotope labelling, is $\frac{1}{\mu}$. Lifetime is defined as the time from cell production, either by division or by entry to the memory compartment, to its death.

We define cell age as the time (in days) since the cell or its ancestor entered the memory compartment, not the time since last division. If we define $w(a,t)$ as the concentration of CD8⁺ T cells of age a at time t. Then
$z(t) = \int_0^\infty w(a,t)da$

The equation for $w(a,t)$, derived from the von Foerster equation[52], is

$$\frac{\partial w}{\partial t} + \frac{\partial w}{\partial a} = \left[s\left(1 - \frac{z}{k}\right) - \mu \right] w \quad (5)$$

with initial condition $w(a,0) = f(a)$, where $f(a)$ is the initial age distribution, and boundary condition $w(0,t) = \lambda$.

We solve the steady-state age distribution by letting $z = \overline{z}$, where bars denote the steady state value. As $\overline{z}$ is a constant, the age equation is of the same form as if there were no proliferation, and a constant death rate equal to $D = \mu - s\left(1 - \frac{\overline{z}}{k}\right)$. Therefore, the age distribution at equilibrium is exponential with rate parameter D, and the mean age is $\frac{1}{D}$.

We can show (Supplementary Results 5), that $\frac{dD}{d\mu} > 0$ for all positive values of model parameters. Therefore, CD8⁺ T cell age increases as CD8⁺ T cell lifetime increases, all other parameters being equal. However, the rate parameter D is the difference of two similar terms both of which might be expected to vary with functional iKIR count and so whilst the intuition that cell age would increase with functional iKIR count due to an increase in cell survival is correct the correlation is expected to be weak.

STATISTICAL ANALYSIS

All statistical analysis was carried out in R version 4.1.2. All reported p values are two tailed, a p value <0.05 was considered significant; where this threshold is decreased due to testing of multiple hypotheses it is noted in the text. Multivariate linear regression, ANOVA, Davidson-MacKinnon J Tests and paired Mann-Whitney tests (Wilcoxon) were conducted with the functions `lm`, `anova`, `lmtest::jtest` and `stats::wilcox.test` respectively (base package unless stated otherwise).

STUDY APPROVAL

All study procedures were conducted according to the principles of the Declaration of Helsinki. All participants gave written informed consent following protocols approved by the national research ethics service (NRES London 13/LO/1621 and 13/LO/0022, South Central Oxford 15/SC/0089/2).

Author Contributions

YZ conducted the experiments. AWCY analysed the data. LB analysed the data and contributed to study design. LH recruited the participants and conducted the experiments. AS conducted the experiments. DPG conducted the experiments. LS analysed the data. LMB analysed the data. NN-G conducted the experiments. JAT supervised the experiments. CR conducted the experiments. DK conducted the experiments. GPT recruited the participants and provided patient data. DF recruited the participants. PJN supervised the experimental work. SGEM supervised the experimental work. RB supervised the experimental work and analysis, contributed to study design and conception. DCM supervised the experimental work, contributed to study design and wrote the manuscript. BA analysed the data, supervised the data analysis, conceptualised and designed the study, acquired funding and wrote the manuscript. Authorship order among co-first authors based on relative contribution of co-author input to the final manuscript.

Acknowledgements

A.W.C.Y is funded by an Imperial College Research Fellowship. J.T. was funded by the European Research Council under the European Union's Horizon 2020 research and innovation program (grant agreement 695551). L.M.B is funded by the European Union H2020 programme under grant agreement 764698 (QUANTII). G.P.T is funded by the National Institute of Health Research Imperial Biomedical Research Centre. P.J.N was funded by NIH NIAID U01 AI090905. D.C.M was partially funded by the Jefferiss Trust. B.A. is a Wellcome Trust (WT) Investigator (103865Z/14/Z) and is also funded by the Medical Research Council (MRC) (J007439, G1001052), the European Union Seventh Framework Programme (FP7/2007–2013) under grant agreement 317040 (QuanTI), the European Union H2020 programme under grant agreement 764698 (QUANTII) and Leukemia and Lymphoma Research (15012). We thank Peter Parham, Stanford University for support during the project, Jyothi Jayaraman, University of Cambridge for technical assistance, Jana Haddow, Specialist Nurse Practitioner, NCHR for her help with recruiting the patients with HTLV-1 and Parisa Amjadi the FACS facility manager at Imperial College London where all CL3 cell sorting was performed.

References

1. Lanier LL. NK CELL RECEPTORS. *Annu Rev Immunol.* 1998;16(1):359-93.
2. Bjorkstrom NK, et al. CD8 T cells express randomly selected KIRs with distinct specificities compared to NK cells. *Blood.* 2012;120(17):3455-65.
3. Zohar O, et al. Cutting edge: MHC class I-Ly49 interaction regulates neuronal function. *J Immunol.* 2008;180(10):6447-51.
4. Robinson J, et al. IPD—the Immuno Polymorphism Database. *Nucleic Acids Res.* 2013;41(D1):D1234-D40.
5. Winter CC, and Long EO. A single amino acid in the p58 killer cell inhibitory receptor controls the ability of natural killer cells to discriminate between the two groups of HLA-C allotypes. *J Immunol.* 1997;158(9):4026-8.
6. Moretta A, et al. Receptors for HLA class-I molecules in human natural killer cells. *Annu Rev Immunol.* 1996;14:619-48.
7. Parham P, and Moffett A. Variable NK cell receptors and their MHC class I ligands in immunity, reproduction and human evolution. *Nat Rev Immunol.* 2013;13(2):133-44.
8. Boelen L, et al. Inhibitory killer cell immunoglobulin-like receptors strengthen CD8(+) T cell-mediated control of HIV-1, HCV, and HTLV-1. *Sci Immunol.* 2018;3(29).
9. Ugolini S, et al. Involvement of inhibitory NKRs in the survival of a subset of memory-phenotype CD8+ T cells. *Nat Immunol.* 2001;2(5):430-5.
10. Diniz MO, et al. NK cells limit therapeutic vaccine–induced CD8+T cell immunity in a PD-L1–dependent manner. *Sci Transl Med.* 2022;14(640):eabi4670.
11. Peppa D, et al. Up-regulation of a death receptor renders antiviral T cells susceptible to NK cell-mediated deletion. *J Exp Med.* 2013;210(1):99-114.
12. Waggoner SN, et al. Natural killer cells act as rheostats modulating antiviral T cells. *Nature.* 2011;481(7381):394-8.
13. Young NT, et al. Differential expression of leukocyte receptor complex-encoded Ig-like receptors correlates with the transition from effector to memory CTL. *J Immunol.* 2001;166(6):3933-41.
14. Piccioli D, et al. Contact-dependent Stimulation and Inhibition of Dendritic Cells by Natural Killer Cells. *J Exp Med.* 2002;195(3):335-41.
15. Pieren DKJ, et al. Regulatory KIR+RA+ T cells accumulate with age and are highly activated during viral respiratory disease. *Aging Cell.* 2021;20(6):e13372.
16. Li J, et al. KIR(+)CD8(+) T cells suppress pathogenic T cells and are active in autoimmune diseases and COVID-19. *Science.* 2022;376(6590):eabi9591.
17. Macallan DC, et al. Current estimates of T cell kinetics in humans. *Curr Opin Syst Biol.* 2019;18:77-86.
18. Costa Del Amo P, et al. Human TSCM cell dynamics in vivo are compatible with long-lived immunological memory and stemness. *PLOS Biol.* 2018;16(6):e2005523.
19. Patel AA, et al. The fate and lifespan of human monocyte subsets in steady state and systemic inflammation. *J Exp Med.* 2017;214(7):1913-23.
20. Akondy RS, et al. Origin and differentiation of human memory CD8 T cells after vaccination. *Nature.* 2017.
21. Vrisekoop N, et al. Sparse production but preferential incorporation of recently produced naive T cells in the human peripheral pool. *Proc Natl Acad Sci U S A.* 2008;105(16):6115-20.
22. Hellerstein MK. Measurement of T-cell kinetics: recent methodologic advances. *Immunol Today.* 1999;20(10):438-41.
23. Busch R, et al. Measurement of cell proliferation by heavy water labeling. *Nat Protoc.* 2007;2(12):3045-57.
24. Alter G, et al. Ligand-independent exhaustion of killer immunoglobulin-like receptor-positive CD8+ T cells in human immunodeficiency virus type 1 infection. *J Virol.* 2008;82(19):9668-77.

25. Laydon DJ, et al. The relative contributions of infectious and mitotic spread to HTLV-1 persistence. *PLOS Comput Biol.* 2020;16(9):e1007470.
26. Wong-Baeza I, et al. KIR3DL2 binds to HLA-B27 dimers and free H chains more strongly than other HLA class I and promotes the expansion of T cells in ankylosing spondylitis. *J Immunol.* 2013;190(7):3216-24.
27. Shaw J, and Kollnberger S. New perspectives on the ligands and function of the killer cell immunoglobulin-like receptor KIR3DL2 in health and disease. *Front Immunol.* 2012;3:339.
28. Chan AT, et al. Expansion and enhanced survival of natural killer cells expressing the killer immunoglobulin-like receptor KIR3DL2 in spondylarthritis. *Arthritis Rheum.* 2005;52(11):3586-95.
29. Huard B, and Karlsson L. KIR expression on self-reactive CD8+ T cells is controlled by T-cell receptor engagement. *Nature.* 2000;403(6767):325-8.
30. Abo T, and Balch CM. A differentiation antigen of human NK and K cells identified by a monoclonal antibody (HNK-1). *J Immunol.* 1981;127(3):1024-9.
31. Ahmed R, et al. CD57(+) Memory T Cells Proliferate In Vivo. *Cell Rep.* 2020;33(11):108501.
32. Roederer M, et al. The Genetic Architecture of the Human Immune System: A Bioresource for Autoimmunity and Disease Pathogenesis. *Cell.* 2015;161(2):387-403.
33. Gossel G, et al. Memory CD4 T cell subsets are kinetically heterogeneous and replenished from naive T cells at high levels. *Elife.* 2017;6.
34. Baliu-Piqué M, et al. Short Lifespans of Memory T-cells in Bone Marrow, Blood, and Lymph Nodes Suggest That T-cell Memory Is Maintained by Continuous Self-Renewal of Recirculating Cells. *Front Immunol.* 2018;9.
35. Hanna GJ, et al. Neoadjuvant and Adjuvant Nivolumab and Lirilumab in Patients with Recurrent, Resectable Squamous Cell Carcinoma of the Head and Neck. *Clin Cancer Res.* 2022;28(3):468-78.
36. Ruggeri L, et al. Effectiveness of donor natural killer cell alloreactivity in mismatched hematopoietic transplants. *Science.* 2002;295(5562):2097-100.
37. Yabe T, et al. Donor killer immunoglobulin-like receptor (KIR) genotype-patient cognate KIR ligand combination and antithymocyte globulin preadministration are critical factors in outcome of HLA-C-KIR ligand-mismatched T cell-replete unrelated bone marrow transplantation. *Biol Blood Marrow Transplant.* 2008;14(1):75-87.
38. Cooley S, et al. Donors with group B KIR haplotypes improve relapse-free survival after unrelated hematopoietic cell transplantation for acute myelogenous leukemia. *Blood.* 2009;113(3):726-32.
39. Mahnke YD, et al. The who's who of T-cell differentiation: human memory T-cell subsets. *Eur J Immunol.* 2013;43(11):2797-809.
40. Ahmed R, et al. Human Stem Cell-like Memory T Cells Are Maintained in a State of Dynamic Flux. *Cell Rep.* 2016;17(11):2811-8.
41. Westera L, et al. Quantitating lymphocyte homeostasis in vivo in humans using stable isotope tracers. *Methods Mol Biol.* 2013;979:107-31.
42. Robinson J, et al. IPD-IMGT/HLA Database. *Nucleic Acids Res.* 2020;48(D1):D948-D55.
43. Bowness P, et al. Th17 cells expressing KIR3DL2+ and responsive to HLA-B27 homodimers are increased in ankylosing spondylitis. *J Immunol.* 2011;186(4):2672-80.
44. Pugh J, et al. Abundant CpG-sequences in human genomes inhibit KIR3DL2-expressing NK cells. *PeerJ.* 2021;9:e12258.
45. Jiang W, et al. qKAT: a high-throughput qPCR method for KIR gene copy number and haplotype determination. *Genome Med.* 2016;8(1):99.
46. Vilches C, et al. Facilitation of KIR genotyping by a PCR-SSP method that amplifies short DNA fragments. *Tissue Antigens.* 2007;70(5):415-22.
47. Norman PJ, et al. Defining KIR and HLA Class I Genotypes at Highest Resolution via High-Throughput Sequencing. *Am J Hum Genet.* 2016;99(2):375-91.

48. Marin WM, et al. High-throughput Interpretation of Killer-cell Immunoglobulin-like Receptor Short-read Sequencing Data with PING. *PLOS Comput Biol.* 2021;17(8):e1008904.
49. Lahoz-Beneytez J, et al. Human neutrophil kinetics: modeling of stable isotope labeling data supports short blood neutrophil half-lives. *Blood.* 2016;127(26):3431-8.
50. Stan_Development_Team. RStan: the R interface to Stan. R package version 2.21.5
51. Soetaert K. R Package FME : Inverse Modelling, Sensitivity,Monte Carlo – Applied to a Dynamic Simulation Model. URL https://cran.r-project.org/web/packages/FME/. v1.3.6.2
52. Murray JD. *Mathematical biology.* New York: Springer; 2002.

Figure Legends

Figure 1. The direct and indirect pathways which could explain iKIR enhancement of $CD8^+$ T cell survival. iKIR (purple) could increase T cell survival and lead to an enhancement of HLA class associations by a number of different pathways. In all diagrams the HLA class I molecule associated with disease outcome is the molecule shown in yellow and labelled "HLA risk molecule" (interacting with the TCR in blue) and the HLA molecule acting as the iKIR ligand is shown in red. (A) Direct hypothesis: iKIR expression on antigen-specific $CD8^+$ T cells reduces activation induced cell death and increases T cell lifespan upon ligation of the cognate KIR ligand. (B) Indirect hypotheses: iKIR ligation on other cells can affect $CD8^+$ T cell lifespan through a range of mechanisms. (1) NK cells can interact with dendritic cells (DCs) and shape downstream T cell responses. (2) NK cells can directly kill activated $CD4^+$ T cells. (3) Similarly, activated $CD8^+$ T cells are also susceptible to NK cell killing. (4) Regulatory KIR^+ $CD8^+$ T cells can kill activated antigen-specific $CD8^+$ T cells.

Figure 2. Percentage of T cells expressing different inhibitory KIR (Cohort 1). The percentage of cells in each subpopulation that expressed each of 3 different iKIR was quantified by flow cytometry for subjects in Cohort 1 (N=23). Multivariate regression found that the following were highly significant predictors of increased iKIR expression: more advanced cell differentiation stage (expressed as an ordinal) $P=4x10^{-14}$, CD8 coexpression P=0.0007 and KIR2DL2/L3 $P=4x10^{-12}$; male gender was weakly predictive (P=0.049). CMV serostatus and infection status were not significant predictors of iKIR expression. Note the scale of the y axis is different between the rows. Boxes show median and interquartile ranges. Data are in Supp Table 1 and the details of the multivariate regression are in Supp Table 2. Number of hypotheses tested=7; p value threshold for $\alpha=0.05$ is P= 0.009 (permutation test).

Figure 3. Label enrichment in $CD8^+$ T cell subpopulations expressing functional iKIR. Plots show, for each individual, the label enrichment in the DNA of sorted T cell subpopulation during and following labelling for 49 days. $CD8^+$ T_{CM} and T_{EMRA} cells were sorted on the basis of their iKIR expression and the individual's HLA ligand genotype into "Func KIR" (Functional iKIR, i.e. expressing a iKIR where the individual carried one or more allele encoding a ligand), "Non Func KIR" (non-functional iKIR, cells expressing iKIR whose ligand is absent from the genome) and "KIR Neg" (not expressing any of the iKIR studied). This figure depicts label enrichment in cells expressing functional iKIR, the remaining data are in Figure 4. Circles represent data and the blue line the best fit of the model to the data. Due to low or absent cell frequencies, it was not possible to collect all cell populations for all individuals.

Figure 4. Label enrichment in $CD8^+$ T cell subpopulations that only express non-functional iKIR or are iKIR-negative. Plots show, for each individual, the label enrichment in the DNA of sorted T cell subpopulation during and following labelling for 49 days. $CD8^+$ T_{CM} and T_{EMRA} cells were sorted on the basis of their iKIR expression and the individual's HLA ligand genotype into "Func KIR" (Functional iKIR, i.e. expressing a iKIR where the individual carried one or more allele encoding a ligand), "Non Func KIR" (non-functional iKIR, cells expressing iKIR whose ligand is absent from the genome) and "KIR Neg" (not expressing any of the iKIR studied). This figure depicts label enrichment in cells expressing only non-functional iKIR or that were iKIR negative, the remaining data are in Figure 3. Circles represent data and the blue line the best

fit of the model to the data. Due to low or absent cell frequencies, it was not possible to collect all cell populations for all individuals.

Figure 5. Predicted and observed relationship between iKIR and T cell Lifespan. A and B are sketches of hypothetical data that depict **predicted** patterns in the data within individuals and between individuals respectively if the direct pathway operates. C and D are sketches of hypothetical data that depict **predicted** patterns within and between individuals if the indirect pathway operates. E and F show the actual **observed** results within and between individuals. E: N=21 paired data sets, F: 53 data points from 18 individuals, boxes show median and interquartile ranges with all individual datapoints superimposed. It can be seen that the observed results are most consistent with the indirect pathway. Note that for the between-individual comparison the T cell lifespan has been adjusted (by linear regression coefficients) to allow for infection status of the individual and for cell subpopulation type (T_{CM} or T_{EMRA}). This is not necessary for the within-individual comparison as this comparison is internally controlled (i.e. both points would be adjusted by the same factor as both points come from the same individual and the same cell subpopulation (T_{CM} or T_{EMRA}). We find that $CD8^+$ T cell lifespan was independent of functional iKIR expression (P=0.79, paired Wilcoxon) and indeed was independent of iKIR expression in general (P=0.50, paired Wilcoxon). In contrast, $CD8^+$ T cell lifespan was significantly determined by iKIR-HLA genotype ($P=3x10^{-6}$, multivariate regression).

Figure 6. CD57 expression increases with the number of functional iKIR genes carried by an individual. T cell subpopulations with measurable CD57 expression (median≥150 events) are plotted. The proportion of cells expressing CD57 was significantly positively correlated with functional iKIR count in $CD4^+$ T_{EM} (P=0.036), $CD8^+$ T_{EM} (P=0.018) and $CD8^+$ T_{EMRA} (P=0.012); multivariate regression with age of the individual as a covariate, N=63. Symbols denote experimental measurements, thin horizontal lines the median CD57 expression (for each subpopulation and each functional iKIR count) and thick lines the best fits line of regression.

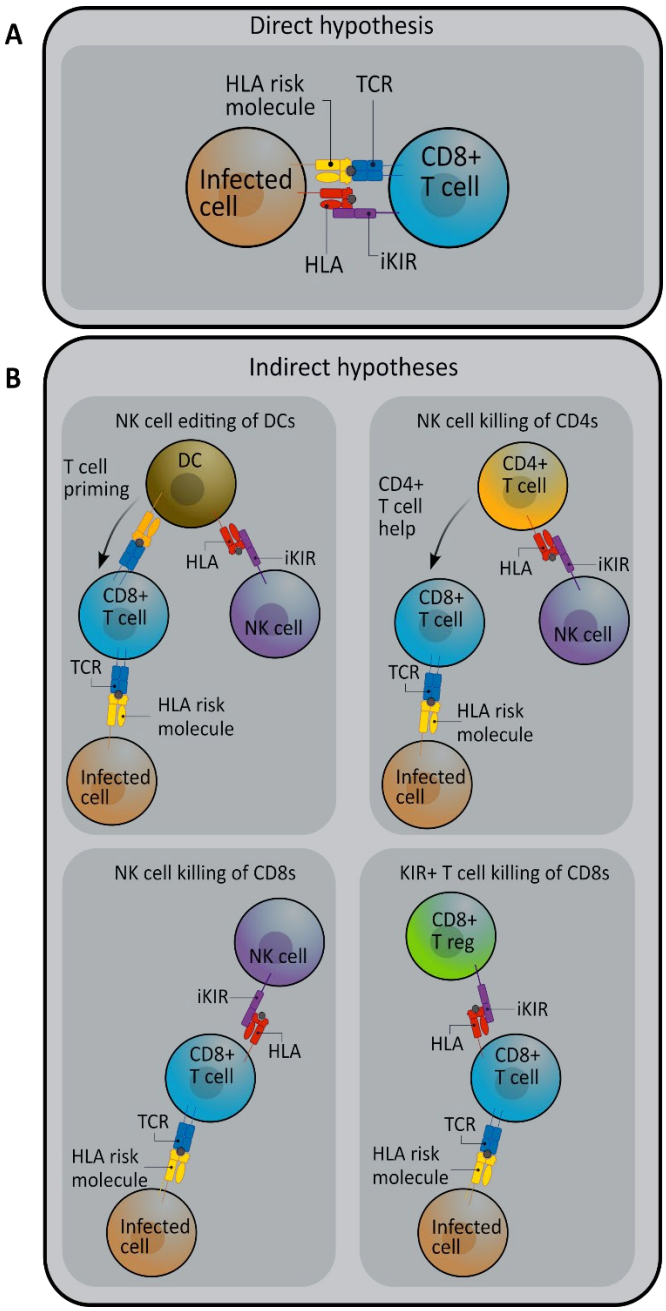

Figure 1. The direct and indirect pathways which could explain iKIR enhancement of CD8⁺ T cell survival. iKIR (purple) could increase T cell survival and lead to an enhancement of HLA class associations by a number of different pathways. In all diagrams the HLA class I molecule associated with disease outcome is the molecule shown in yellow and labelled "HLA risk molecule" (interacting with the TCR in blue) and the HLA molecule acting as the iKIR ligand is shown in red. (A) Direct hypothesis: iKIR expression on antigen-specific CD8⁺ T cells reduces activation induced cell death and increases T cell lifespan upon ligation of the cognate KIR ligand. (B) Indirect hypotheses: iKIR ligation on other cells can affect CD8⁺ T cell lifespan through a range of mechanisms. (1) NK cells can interact with dendritic cells (DCs) and shape downstream T cell responses. (2) NK cells can directly kill activated CD4⁺ T cells. (3) Similarly, activated CD8⁺ T cells are also susceptible to NK cell killing. (4) Regulatory KIR⁺ CD8⁺ T cells can kill activated antigen-specific CD8⁺ T cells.

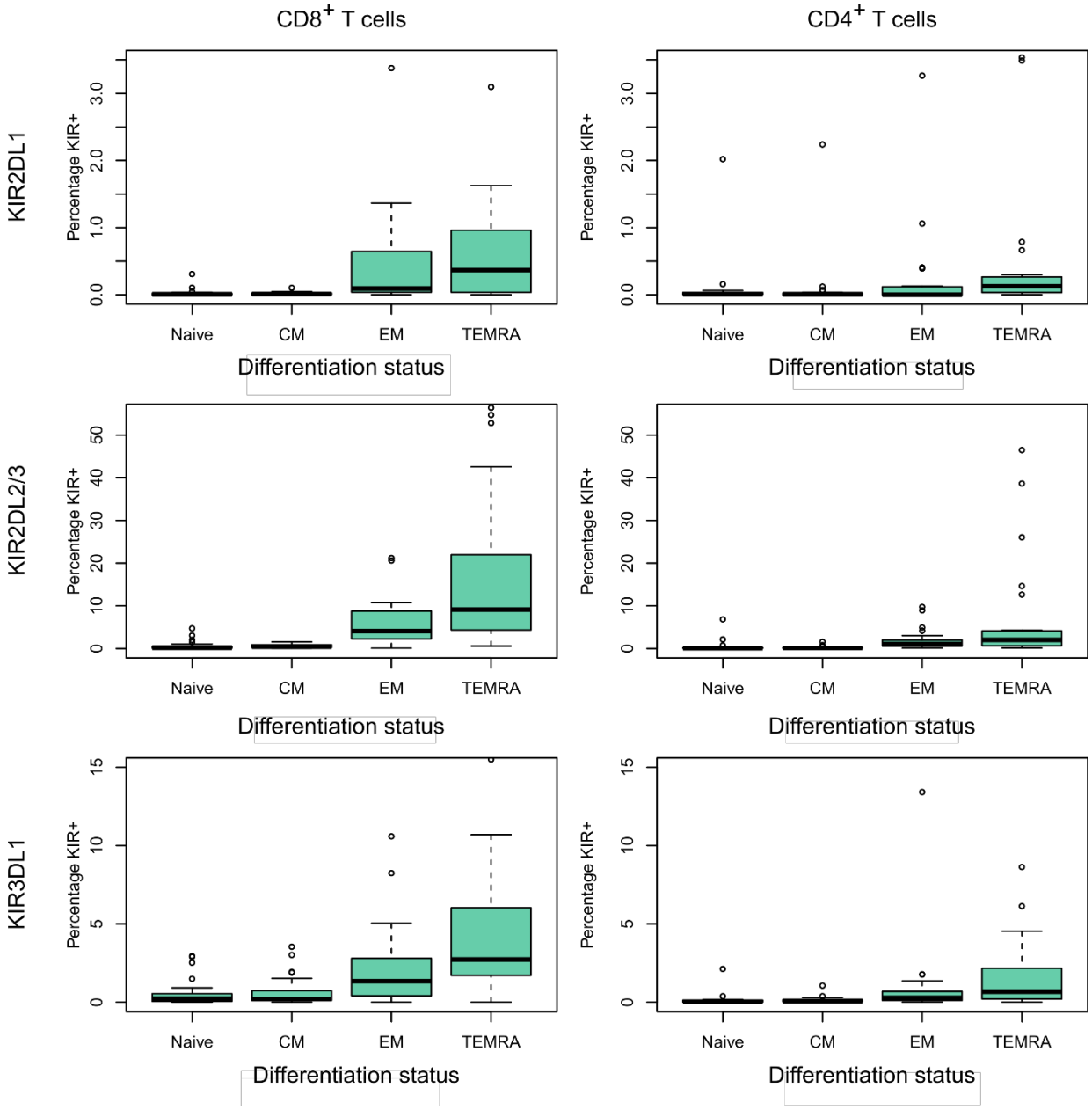

Figure 2. Percentage of T cells expressing different inhibitory KIR (Cohort 1). The percentage of cells in each subpopulation that expressed each of 3 different iKIR was quantified by flow cytometry for subjects in Cohort 1 (N=23). Multivariate regression found that the following were highly significant predictors of increased iKIR expression: more advanced cell differentiation stage (expressed as an ordinal) $P=4x10^{-14}$, CD8 coexpression P=0.0007 and KIR2DL2/L3 $P=4x10^{-12}$; male gender was weakly predictive (P=0.049). CMV serostatus and infection status were not significant predictors of iKIR expression. Note the scale of the y axis is different between the rows. Boxes show median and interquartile ranges. Data are in Supp Table 1 and the details of the multivariate regression are in Supp Table 2. Number of hypotheses tested=7; p value threshold for $\alpha=0.05$ is P= 0.009 (permutation test).

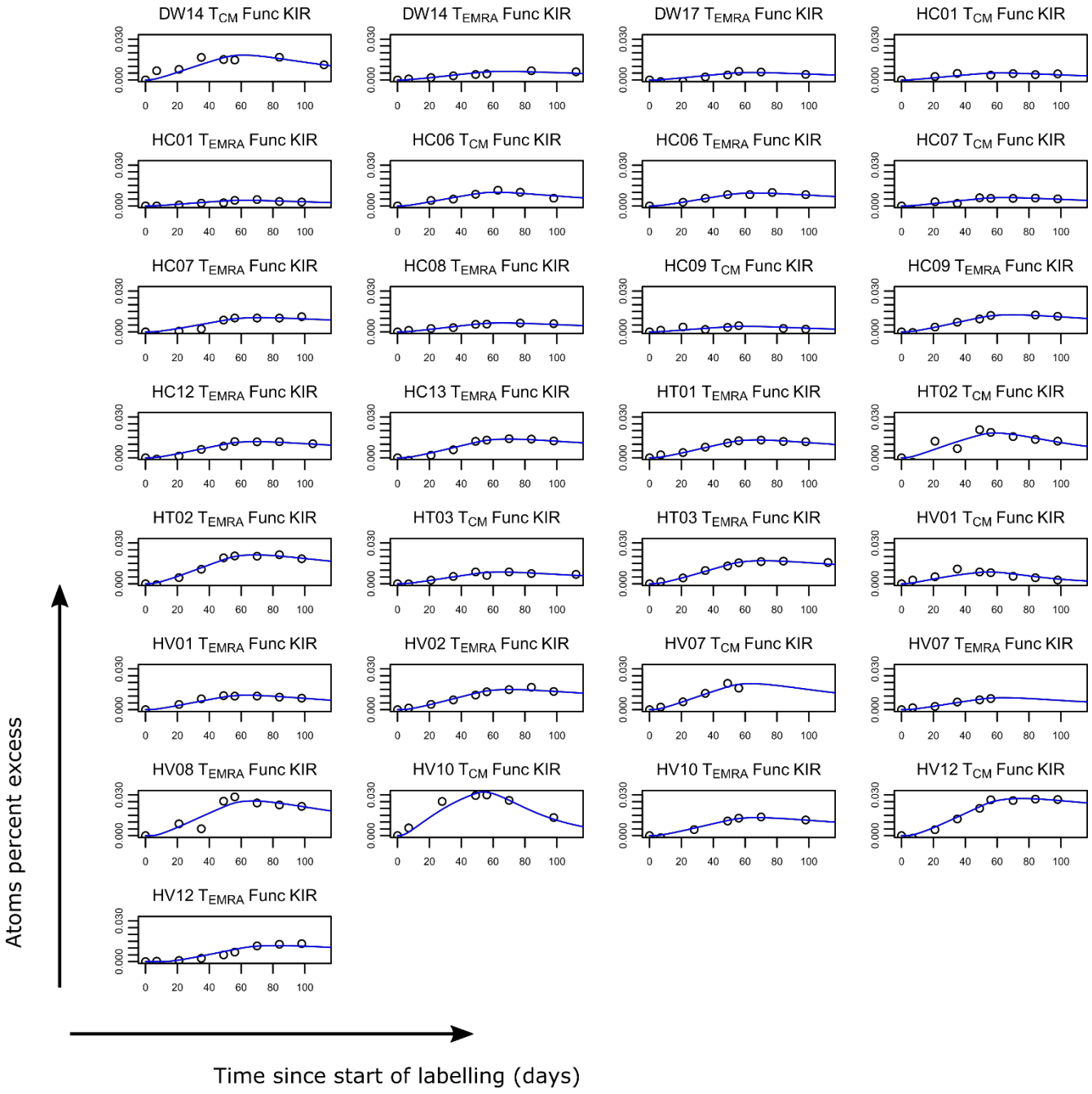

Figure 3. Label enrichment in CD8⁺ T cell subpopulations expressing functional iKIR. Plots show, for each individual, the label enrichment in the DNA of sorted T cell subpopulation during and following labelling for 49 days. CD8⁺ T_{CM} and T_{EMRA} cells were sorted on the basis of their iKIR expression and the individual's HLA ligand genotype into "Func KIR" (Functional iKIR, i.e. expressing a iKIR where the individual carried one or more allele encoding a ligand), "Non Func KIR" (non-functional iKIR, cells expressing iKIR whose ligand is absent from the genome) and "KIR Neg" (not expressing any of the iKIR studied). This figure depicts label enrichment in cells expressing functional iKIR, the remaining data are in Figure 4. Circles represent data and the blue line the best fit of the model to the data. Due to low or absent cell frequencies, it was not possible to collect all cell populations for all individuals.

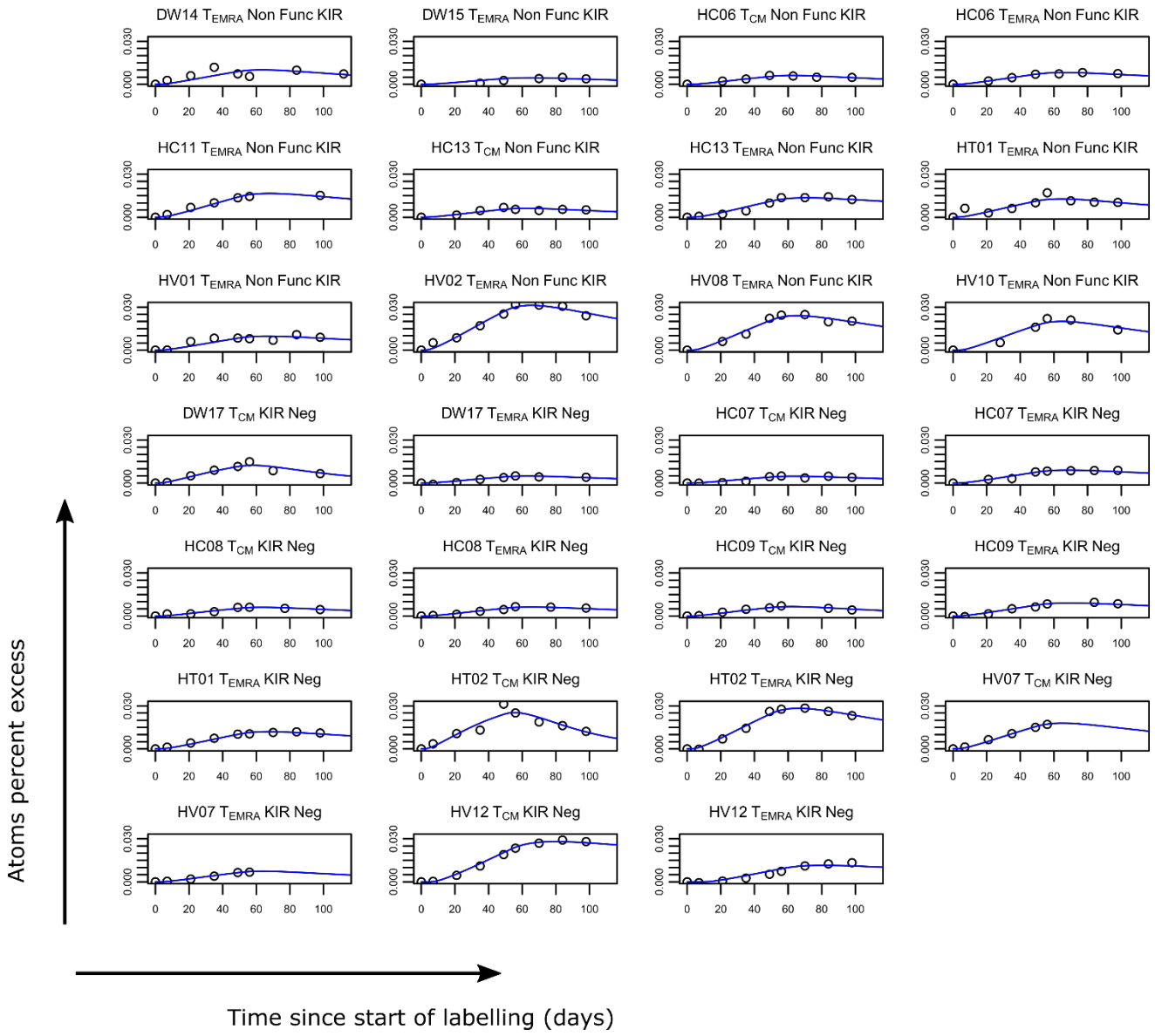

Figure 4. Label enrichment in CD8⁺ T cell subpopulations that only express non-functional iKIR or are iKIR-negative. Plots show, for each individual, the label enrichment in the DNA of sorted T cell subpopulation during and following labelling for 49 days. CD8⁺ T_{CM} and T_{EMRA} cells were sorted on the basis of their iKIR expression and the individual's HLA ligand genotype into "Func KIR" (Functional iKIR, i.e. expressing a iKIR where the individual carried one or more allele encoding a ligand), "Non Func KIR" (non-functional iKIR, cells expressing iKIR whose ligand is absent from the genome) and "KIR Neg" (not expressing any of the iKIR studied). This figure depicts label enrichment in cells expressing only non-functional iKIR or that were iKIR negative, the remaining data are in Figure 3. Circles represent data and the blue line the best fit of the model to the data. Due to low or absent cell frequencies, it was not possible to collect all cell populations for all individuals.

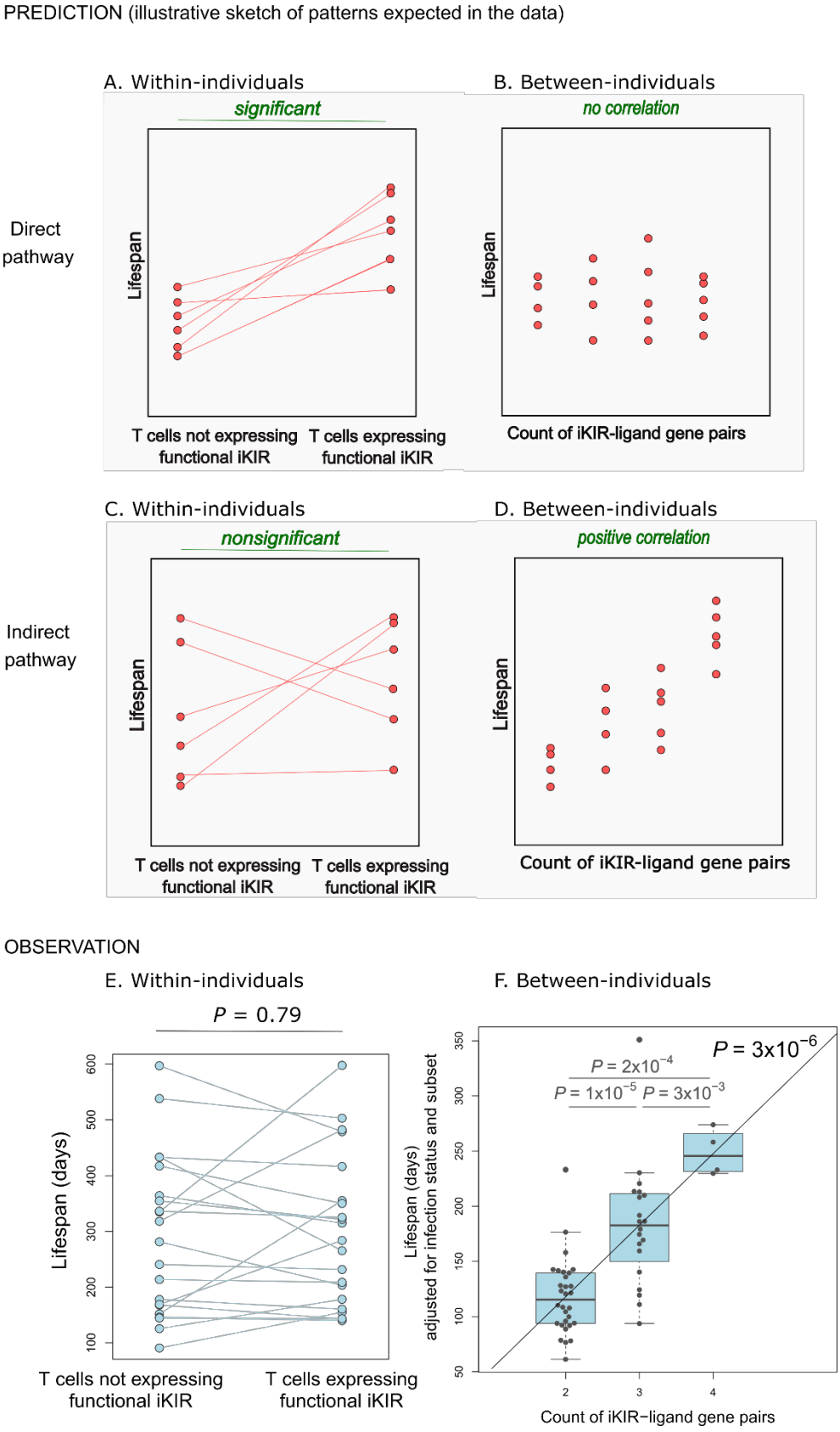

Figure 5. Predicted and observed relationship between iKIR and T cell Lifespan. A and B are sketches of hypothetical data that depict **predicted** patterns in the data within individuals and between individuals respectively if the direct pathway operates. C and D are sketches of

hypothetical data that depict **predicted** patterns within and between individuals if the indirect pathway operates. E and F show the actual **observed** results within and between individuals. E: N=21 paired data sets, F: 53 data points from 18 individuals, boxes show median and interquartile ranges with all individual datapoints superimposed. It can be seen that the observed results are most consistent with the indirect pathway. Note that for the between-individual comparison the T cell lifespan has been adjusted (by linear regression coefficients) to allow for infection status of the individual and for cell subpopulation type (T_{CM} or T_{EMRA}). This is not necessary for the within-individual comparison as this comparison is internally controlled (i.e. both points would be adjusted by the same factor as both points come from the same individual and the same cell subpopulation (T_{CM} or T_{EMRA}). We find that $CD8^+$ T cell lifespan was independent of functional iKIR expression (P=0.79, paired Wilcoxon) and indeed was independent of iKIR expression in general (P=0.50, paired Wilcoxon). In contrast, $CD8^+$ T cell lifespan was significantly determined by iKIR-HLA genotype ($P=3x10^{-6}$, multivariate regression).

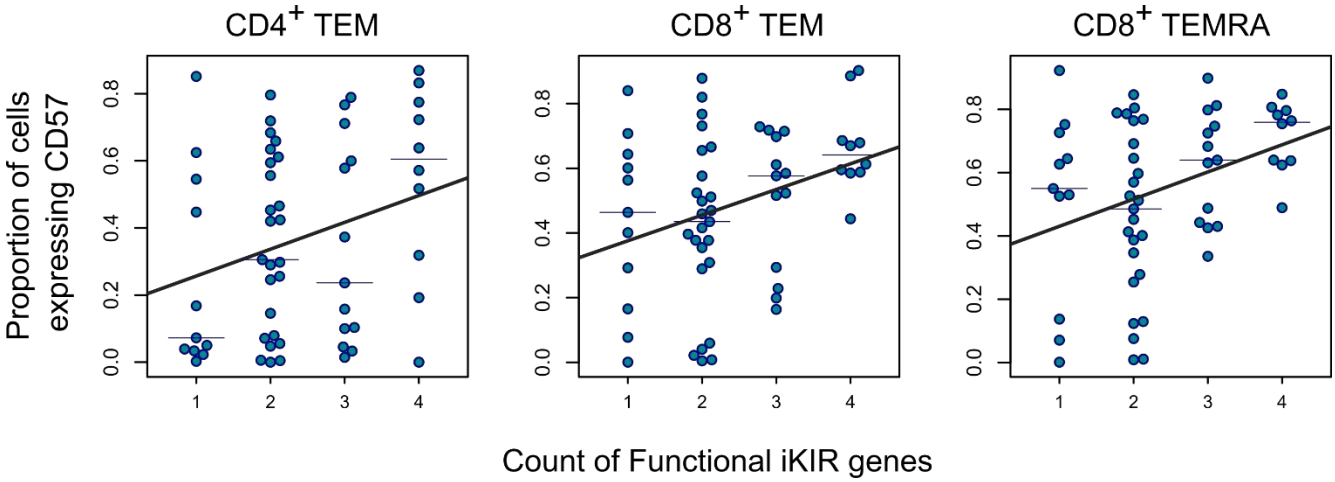

Figure 6. CD57 expression increases with the number of functional iKIR genes carried by an individual. T cell subpopulations with measurable CD57 expression (median≥150 events) are plotted. The proportion of cells expressing CD57 was significantly positively correlated with functional iKIR count in $CD4^+$ T_{EM} (P=0.036), $CD8^+$ T_{EM} (P=0.018) and $CD8^+$ T_{EMRA} (P=0.012); multivariate regression with age of the individual as a covariate, N=63. Symbols denote experimental measurements, thin horizontal lines the median CD57 expression (for each subpopulation and each functional iKIR count) and thick lines the best fits line of regression.